lubricants

MDPI

Article

Optimizing the Artificial Aging Process of Lubricating Oils Contaminated by Alternative Fuel Using Design of Experiments Methodology

Dominika Pintér * and András Lajos Nagy

Department of Propulsion Technology, Széchenyi István University, Egyetem tér 1, H-9026 Győr, Hungary; nagy.andras1@sze.hu

* Correspondence: pinter.dominika@sze.hu

Abstract

This study aimed to develop an experimental method for producing artificially aged oil with properties—such as coefficient of friction, average wear scar diameter, and antiwear additive content—similar to those of used oil contaminated with alternative fuel, sampled after 129 h of engine test bench operation. A design of experiment (DoE) methodology was applied to examine the effects of various parameters and identify optimal settings. Friction and wear tests were conducted using an Optimol SRV5 tribometer in a ball-on-disc configuration, while wear scars were analyzed with a Keyence VHX-1000 digital microscope. Oil analysis was conducted with an Anton Paar 3001 viscometer and a Bruker Invenio-S Fourier-transform infrared spectrometer. The DoE results showed that the heating duration had a negligible effect on oil degradation. Aging time primarily affected changes in the friction coefficient and average wear scar diameter, whereas aging temperature was the primary factor influencing the anti-wear additive content. Gaussian elimination identified the optimal aging parameters as 132.8 °C and 103.1 h. These results were confirmed through surface analysis using a ThermoFisher NexsaG2 X-ray photoelectron spectrometer, which showed that the tribofilm composition of the used oil most closely matched that of artificially aged oils prepared at 120 °C for 96 h and 140 °C for 120 h. The strong correlation between the predicted and experimentally confirmed conditions demonstrates the reliability of the proposed method for replicating realistic aging effects in lubricating oils.

Keywords: design of experiment; artificial oil aging; coefficient of friction; wear scar diameter; alternative fuel; ZDDP; XPS

check for updates

Received: 31 July 2025
Revised: 1 September 2025
Accepted: 9 September 2025
Published: 11 September 2025

Citation: Pintér, D.; Nagy, A.L. Optimizing the Artificial Aging Process of Lubricating Oils Contaminated by Alternative Fuel Using Design of Experiments Methodology. *Lubricants* **2025**, *13*, 405. https://doi.org/10.3390/lubricants13090405

Copyright: © 2025 by the authors. Licensee MDPI, Basel, Switzerland. This article is an open access article distributed under the terms and conditions of the Creative Commons Attribution (CC BY) license (https://creativecommons.org/licenses/by/4.0/).

1. Introduction

In recent years, the automotive industry has undergone significant changes due to environmental protection efforts. As a result of global regulations aimed at reducing harmful emissions, the development of electric vehicles has become more prominent. However, in applications where electric cars are not suitable because of inadequate charging infrastructure or limited battery range, hybrid and internal combustion engine (ICE) vehicles may serve as practical alternatives [1–3]. Consequently, the development and optimization of internal combustion engines remain critically important, especially for reducing emissions and enhancing fuel efficiency [4]. Along with engine downsizing [5,6], testing alternative fuels has also become a significant focus of research [7,8]. Achieving these development goals

requires investigating internal combustion engines, where engine test bench experiments play a crucial role. However, such testing involves significant costs and environmental impact due to high fuel and lubricant consumption, as well as engine emissions.

One alternative is the use of tribometer-based tests for pre-screening, which enable the study of friction and wear processes under laboratory conditions using standard test specimens [9,10], specimens resembling engine components, or actual engine parts [11,12]. However, this method may only serve as a substitute for online wear measurement procedures, as the oils used in these experiments are typically still sourced from engine bench tests, which employ used oils from real engine applications [13,14]. A potential solution to this problem is artificial oil aging, where the lubricant is degraded under laboratory or industrial conditions through various types of stress. Artificial oil aging usually involves thermo-oxidative modification, which can be conducted according to standardized procedures at ambient or elevated pressures, with or without the use of metal catalysts [15–18]. Nonetheless, standardized methods do not always fully replicate the properties of used oils. In internal combustion engines, oil aging is influenced not only by high temperatures and oxidation but also by the presence of fuel—especially combustion products of ethanol [19,20], soot contamination [21], and nitration [22]. Therefore, these factors must be considered during artificial aging, especially when examining their individual or combined effects.

To assess whether artificially aged oils have undergone sufficient degradation, key indicators are typically evaluated, including changes in viscosity, the extent and type of oxidation, and the depletion of additives such as the antiwear compound ZDDP (zinc dialkyldithiophosphate). Studies have shown that the degradation level of ZDDP due to artificial aging significantly impacts the composition and thickness of the antiwear tribofilm [23], and that it differs from the tribological boundary layers created by fresh and in-service oils [24]. Cen et al. found that aging at lower temperatures led to reduced wear compared to fresh oils [25]. By comparing aged oils with in-service samples, Nagy et al. concluded that artificial aging of motor oil for 96 h at 180 °C resulted in oil properties similar to those after 7000 km of mixed driving conditions [19]. Besser et al. reported a high degree of chemical similarity between artificially aged and target used oil samples, not only in conventional oil parameters but also in the structure of ZDDP and nitration degradation products [22]. Additionally, they confirmed a remarkable similarity in the chemical composition of large-scale artificially aged samples and the selected reference used oils, including additive decomposition and the formation of degradation products [26].

One of the characteristic parameters of ZDDP performance is the formation of the tribofilm on metal surfaces under boundary lubrication conditions. Its composition, thickness, and stability are critical for antiwear protection. These properties are mainly studied with surface-sensitive methods, most commonly X-ray photoelectron spectroscopy (XPS). XPS reveals both the elemental composition and the chemical states of phosphorus, sulfur, and zinc, allowing the distinction between short- and long-chain phosphates as well as sulfide and sulfate species [27–29]. Depth profiling with XPS also provides information on the layered structure of the film and its overall thickness. Several studies have demonstrated that the level of degradation of ZDDP—whether resulting from actual engine use or artificial aging—significantly impacts these parameters. Thornley [30] reported that artificially aged oils exhibited delayed or minimal ZDDP tribofilm growth, while engine-aged oils performed similarly to fresh oils without friction modifiers. Under real engine conditions, ZDDP was observed to decompose into nanoscale ZnO particles enriched with phosphorus and sulfur [31]. In sooted oils, only a thin sulfide layer formed instead of a complete tribofilm, supporting a tribocorrosive wear mechanism, whereas centrifuged oils allowed typical ZDDP films to develop [32]. Other studies confirmed that oil degradation changes

tribofilm chemistry, with sulfides decreasing and sulfates increasing, along with declining levels of zinc, phosphorus, and sulfur—changes linked to both reduced wear rates and decreased film stability [33,34].

The aim of this research is to investigate how various parameters influence artificial oil aging, with the goal of identifying those that have a significant impact on lubricant degradation. Furthermore, the study aims to find artificial aging conditions that closely match the properties of a used oil sample collected from an engine test bench after 129 h of operation. The novelty of this work lies in the development of a systematic and optimized approach for artificial oil aging, where a design of experiment (DoE) methodology is combined with Gaussian elimination to identify the most influential parameters and determine optimal conditions. Unlike previous studies, the present work not only relies on chemical characterization but also validates the aging results through surface analysis of tribofilms formed during friction tests. This approach provides the opportunity to simulate the degradation of lubricants contaminated with alternative fuels under laboratory conditions, offering a practical and cost-effective alternative to engine test bench experiments.

2. Materials and Methods

In this study, the friction and wear properties of used SAE 0W-20 engine oil (Shell Helix Ultra, Shell, London, UK) and several artificially aged SAE 0W-20 lubricants contaminated with alternative fuel are observed, along with analyses of viscosity and oil spectra, with particular focus on ZDDP content. The evaluation of the coefficient of friction, average wear scar diameter, and changes in ZDDP (zinc dialkyldithiophosphate) content was performed using a design of experiments (DoE) approach. An additional goal was to identify which conditions of artificial oil aging most closely resemble the properties of used oil. The used oil sample was collected after 129 h of engine bench testing under durability conditions similar to the test cycle detailed in [35]. For the artificially aged oils, a thermo-oxidative process was employed, varying the aging temperature, the length of each heating cycle, and the total aging duration. The evaluation and verification of the results were performed through surface analytical measurements on the selected specimens.

2.1. Design of Experiment—Fractional Factorial

A design of experiments (DoE) methodology was applied in this study to maximize the information gained from a limited number of tests. The primary aim was not to develop a predictive model, but rather to map the effects of selected parameters and determine the extent to which each variable influences the system's response. Based on this objective, a fractional factorial design was chosen. Three variables were defined for the tests—temperature (A), heating period (B), and aging time (C)—each set at three levels, while all other parameters were held constant. Previous research has indicated [19] that aging at 180 °C with 12 h heating cycles for a total of 96 h results in the depletion of the anti-wear additive ZDDP, leading to increased wear scar diameters. However, since the goal was to simulate oil conditions comparable to those of a used sample collected after 129 h of engine bench operation, this aging setting was deemed excessively severe. Consequently, the upper temperature level was set at 160 °C, and the lower limit at 120 °C, as ZDDP is thermally stable below this threshold and does not degrade. The mid-level for the heating period was maintained at 12 h, while the lower and upper bounds were set at 6 and 24 h, respectively, for practical reasons. Based on earlier findings, temperature was expected to be the most influential factor affecting oil degradation, followed by total aging time. Therefore, the maximum aging duration was set at 96 h, consistent with previous studies. The five selected aging conditions for the artificial aging procedure are illustrated in Figure 1.

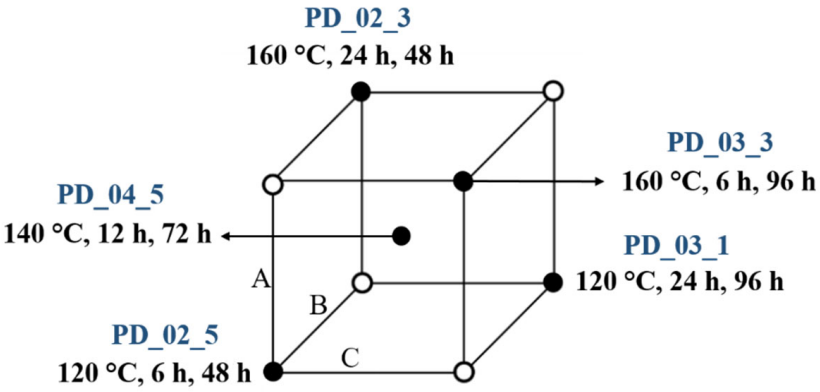


Figure 1. Fractional factorial design showing aging temperature (A), heating period (B), and ageing time (C).

2.2. Artificial Oil Aging Methodology

The artificial oil aging experiments were conducted using a custom-designed aging apparatus developed by the Department of Propulsion Technology at Széchenyi István University [36], as shown in Figure 2.



Figure 2. Custom-designed oil aging device.

The primary aim of the setup was to simulate the degradation effects observed in used oils by subjecting fresh 0W-20 grade lubricants to thermal stress and oxidation. Air was supplied from the building's centralized compressed air system at 2 bars, with a flow rate maintained at 1 L/min, monitored using rotameters. As outlined in Section 2.1, three key variables were defined in addition to the fixed parameters: temperature (A), heating period (B), and total aging time (C). Each heating cycle was followed by a cooling period of equal duration at room temperature. These cycles alternated until the total aging time was reached. Additionally, to reproduce the chemical conditions of the engine bench test, the oils were contaminated with an experimental E20 fuel (20% ethanol by volume), as this same alternative fuel had been used in the real engine tests. The contamination level was set at 10 m/m% and distributed proportionally across the number of heating cycles.

Specifically, the E20 fuel was introduced during the final hour of each cooling period. For example, in sample PD_02_5, the 6 h heating period was repeated twice over a total aging time of 48 h, and the oil was contaminated with 2 × 5 m/m% E20 fuel. The repeatability of the artificial aging procedure was verified at one experimental point, with the results summarized in Table 1.

Table 1. Evaluation of the repeatability of the artificial oil-aging apparatus under duplicate aging conditions.

	Average Wear Scar Diameter [µm]	Coefficient of Friction [-]	Kinematic Viscosity at 100 °C [mm/s^2]
PD_02_5	572	0.1496	8.029
PD_03_5	570.8	0.1465	8.0162
Variation	0.21%	2.16%	0.16%

2.3. Friction and Wear Tests

Friction and wear tests were conducted using an Optimol SRV5 oscillating tribometer (Optimol Instruments Prüftechnik GmbH, Munich, Germany) in a ball-on-disc configuration as shown in Figure 3.

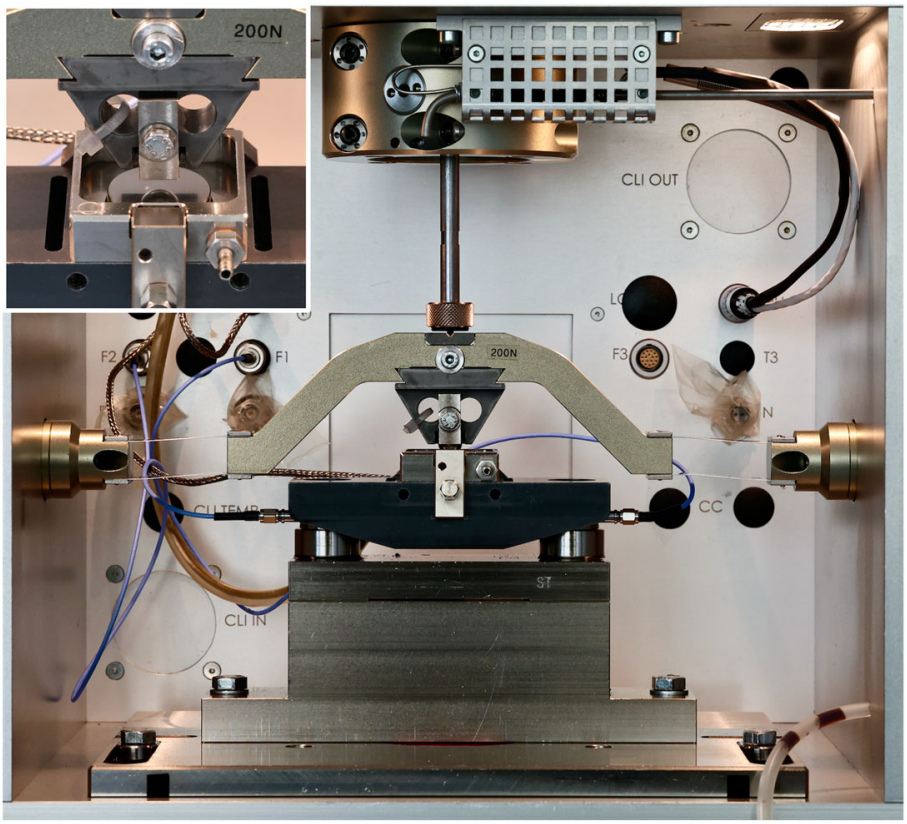


Figure 3. Optimol SRV5 oscillating tribometer in a ball-on-disc configuration.

The tests were performed using a point contact arrangement with a 10 mm diameter ball against a 24 mm diameter, 7.9 mm thick disc, both made of 100Cr6 bearing steel as suggested in ISO 19291:2016(E) [37]. All experiments were carried out at a temperature of 100 °C under a normal load of 150 N, an oscillation frequency of 50 Hz, and a stroke length of 1 mm. The selected load condition results in an approximately 339 µm Hertzian contact diameter. Based on the parameters applied in the tribometer experiments, the

minimum oil film thickness was calculated using the Hamrock–Dowson equation [38] for the oils with the lowest and highest dynamic viscosity values, resulting in 6.46 and 6.48 nanometers, respectively. Considering the ratio of the calculated oil film thickness to the surface roughness of the disc (Ra = 0.047 µm), the obtained λ value was 0.13. According to the Stribeck curve, this indicates that the measurements were conducted in the boundary lubrication regime. A continuous oil circulation system provided lubrication at a flow rate of 2.25 mL/h. Each test lasted a total of 60 min, including a 5 min running-in phase at a reduced load of 50 N. The coefficient of friction (CoF) was recorded using high-speed data acquisition. For evaluation purposes, the average CoF value over the first 5 s of the 30th minute of the test was considered, as this was found to be representative of the entire test duration in all cases, as demonstrated in Table 2. The only exception was the running-in phase, during which the coefficient of friction (CoF) could reach up to three times its steady-state value. Each oil sample was tested three times to assess repeatability. The characteristic coefficient of friction for a given oil condition was calculated as the average of these three measurements.

Table 2. The variation in the coefficient of friction across four time intervals. In all cases, the variation between data from different time intervals was smaller than the variation among the three repeated measurements.

PD_02_3	30:00–30:05	30:00–35:00	55:00–55:05	55:00–60:00	Variation
Measurement 1	0.137	0.139	0.14	0.138	0.12%
Measurement 2	0.144	0.144	0.142	0.144	0.1%
Measurement 3	0.139	0.139	0.14	0.141	0.07%
Variation	2.42%	1.78%	0.76%	2.0%	-

2.4. Wear Analysis

The wear scars were analyzed using a Keyence VHX-1000 digital microscope (Keyence International, Mechlin, Belgium), equipped with a VH-Z100R objective lens. A 100× magnification was applied to the disc specimens, and a 200× magnification was applied to the ball specimens. The average wear scar diameters were evaluated in accordance with ISO 19291:2016(E) [37] by measuring the length and width of the wear marks on the ball specimens parallel and perpendicular to the wear direction, as illustrated in Figure 4.

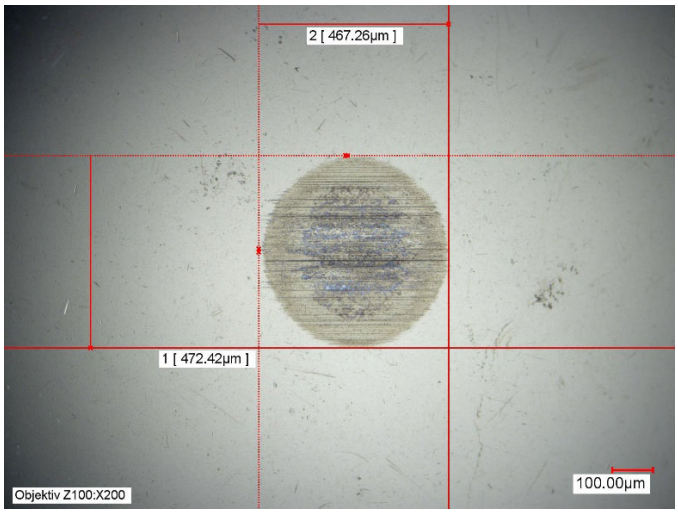


Figure 4. Wear scar on the ball specimen with dimensional annotation.

2.5. Oil Analysis

Following the analysis of friction and wear parameters, oil characterization was performed using an Anton Paar SVM 3001 viscometer (Anton Paar GmbH, Graz, Austria) and a Bruker INVENIO-S Fourier-transform infrared (FT-IR) spectrometer (Bruker Corporation, Billerica, MA, USA). The density and kinematic viscosity of the oils were measured at 40 °C and 100 °C in accordance with the ASTM D7042-21 standard [39]. FT-IR spectroscopy was employed to determine changes in anti-wear additive content and to compare oil spectra. While this method is generally not suitable for determining absolute concentration, it becomes quantifiable when a reference oil is available for comparison. Accordingly, the change in anti-wear additive content was determined based on the principle of spectral subtraction, as outlined in ASTM E2412-10R [40].

2.6. Surface/Tribofilm Analysis

Surface analytical characterization of the disc specimens was performed using a Thermo Scientific Nexsa G2 X-ray photoelectron spectrometer (Thermo Fisher Scientific, Waltham, MA, USA) equipped with a monochromatic Al Kα (1486.6 eV) X-ray source. Measurements were conducted using a focused spot size of 100 µm in diameter. The analysis was carried out in line scan mode, where the atomic percentages of selected elements—namely Zn and P—were measured uniformly at 20 steps along the wear scar. Data evaluation was performed using the Smart peak fitting algorithm.

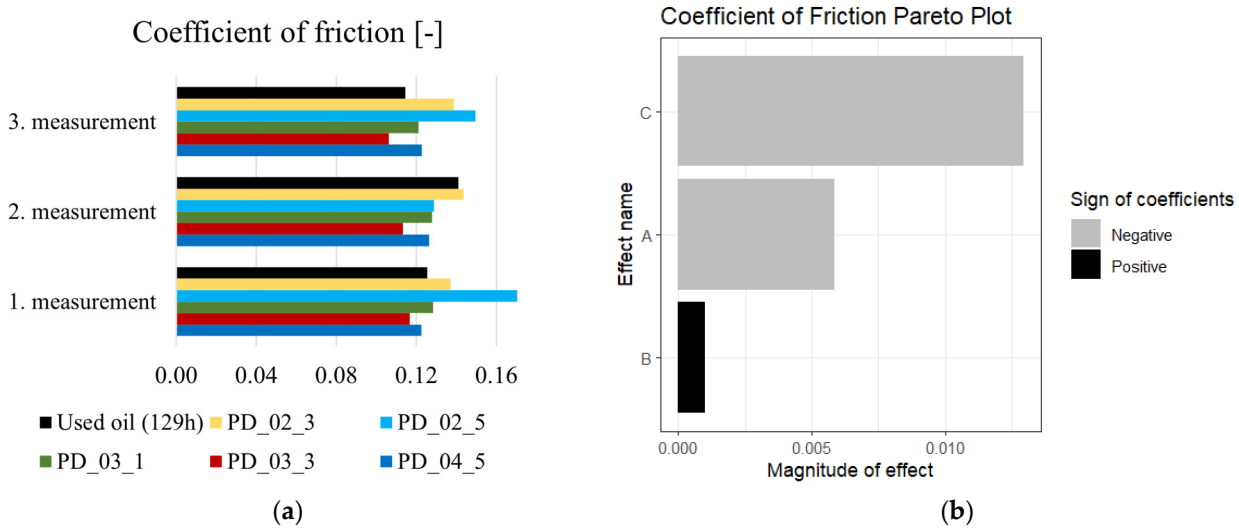
3. Results and Discussion

Based on the quantified values of the friction coefficient, average wear scar diameter, and changes in anti-wear additive content obtained during the experiments, three distinct linear models were constructed using a fractional factorial design.

3.1. CoF Results

The analysis of the friction coefficient values, as illustrated in Figure 5a, primarily demonstrates that, when dealing with large datasets, graphical representation through charts does not always provide transparent and easily interpretable information. The application of design of experiment methodologies is crucial not only due to their cost- and time-efficiency but also because they offer a comprehensive overview of which variables exert the most significant influence on the given system. The results showed that the oil labeled PD_02_5 exhibited an outlier value during the first measurement, which could have led to the mistaken conclusion that the sample preparation was inadequate. However, as detailed in Section 2.2 regarding the repeatability check of the aging apparatus, this oil served as the reference. It showed only a 2% deviation compared to the oil aged under identical conditions, indicating that the outlier values were not due to preparation errors. Furthermore, the oils labeled PD_02_3 and PD_02_5 exhibited the highest friction coefficients during the measurements, both of which shared a common factor: a 48 h aging duration.

The lowest friction coefficient was observed for the oil labeled PD_03_3, which was aged at a relatively high temperature of 160 °C for 96 h. Initially, this indicated that shorter aging durations resulted in higher friction coefficients, whereas more extended aging periods led to lower coefficients. Despite different setting parameters, the oils PD_03_1 and PD_04_5 had nearly identical friction coefficients, emphasizing the importance of experimental design in understanding the system's behavior. The Pareto analysis (Figure 5b) showed that variations in the heating period (B) had a negligible impact on the changes within the system. In contrast, the aging time (C) had the most substantial impact.

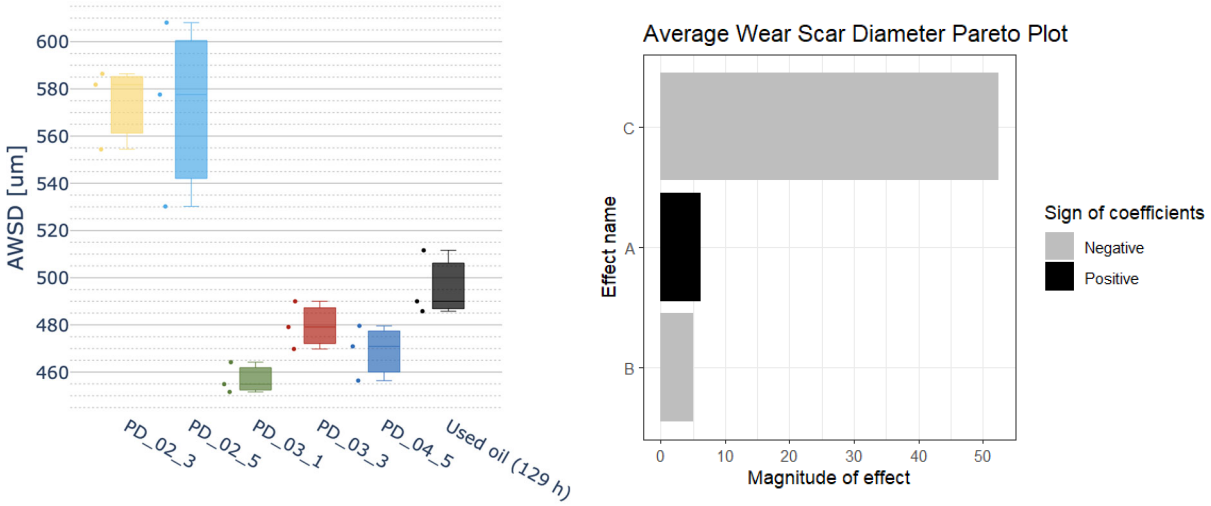


(**a**) (**b**)

Figure 5. (**a**) Changes in friction coefficients of the tested oils; (**b**) Pareto analysis of the model constructed based on friction coefficients.

3.2. AWSD Results

The variation in average wear scar diameter values of the ball specimens for each oil is presented in Figure 6a. The largest average wear scar diameters were characteristic of oils labeled PD_02_3 and PD_02_5. The highest variability was also observed for the PD_02_5 oil, reaching nearly 40 µm in diameter. Similar to the friction coefficient, a significant influence of aging time on the system was also assumed here, as longer aging durations resulted in smaller average wear scar diameters and reduced variability. The lowest average wear scar diameter was recorded for the PD_03_1 oil, with the slightest variation of 6.5 µm. The oil marked PD_03_3 exhibited the largest wear scar diameter, likely because PD_03_3 was aged at the highest temperature (160 °C), suggesting that wear scar size was influenced not only by aging time. Despite this, Figure 6b shows that aging time is a significant variable, while the effect of heating period was again considered negligible.



(**a**) (**b**)

Figure 6. (**a**) Evolution of average wear scar diameter values for the investigated oils; (**b**) Pareto analysis of the model constructed based on average wear scar diameter values.

3.3. Oil Analysis Results

To investigate the changes in friction coefficients and average wear scar diameters, an analysis of the tested lubricants was also conducted. Initially, the oils were examined using a viscometer in accordance with ASTM D7042-21 [39] at temperatures of 40 and 100 °C. No significant differences were observed in kinematic viscosity and density among the oils that could explain the variations in friction coefficients and wear scar diameters. When comparing the kinematic viscosity values, differences of 0.8% at 40 °C and 0.13% at 100 °C were found among the artificially aged oils, indicating that thermo-oxidative aging either did not affect the viscosity modifier additive or had a similar effect on all oils. Density differences were an order of magnitude smaller, with only 0.02% deviation at both 40 and 100 °C.

The quantification of anti-wear additive depletion in artificially aged and used oils was performed by creating difference spectra using a 0W20 viscosity grade reference oil. Each oil's spectrum was subtracted from the reference oil spectrum to generate the difference spectra. According to ASTM E2412-10 [40], the anti-wear additive is identified within the 1020–930 cm^{-1} wavenumber range. The amount of anti-wear additive was determined by measuring the perpendicular height between the baseline fitted to two points on the difference spectrum and the highest point within the 1020–930 cm^{-1} range, expressed as Abs/0.1 mm. The greater this value, the more depleted the anti-wear additive content, as the difference spectra reflect changes in additive concentration. Figure 7a illustrates these changes in the tested lubricants using difference spectra. It is visible that the most significant changes occurred in the oils labeled PD_02_3 and PD_03_3.

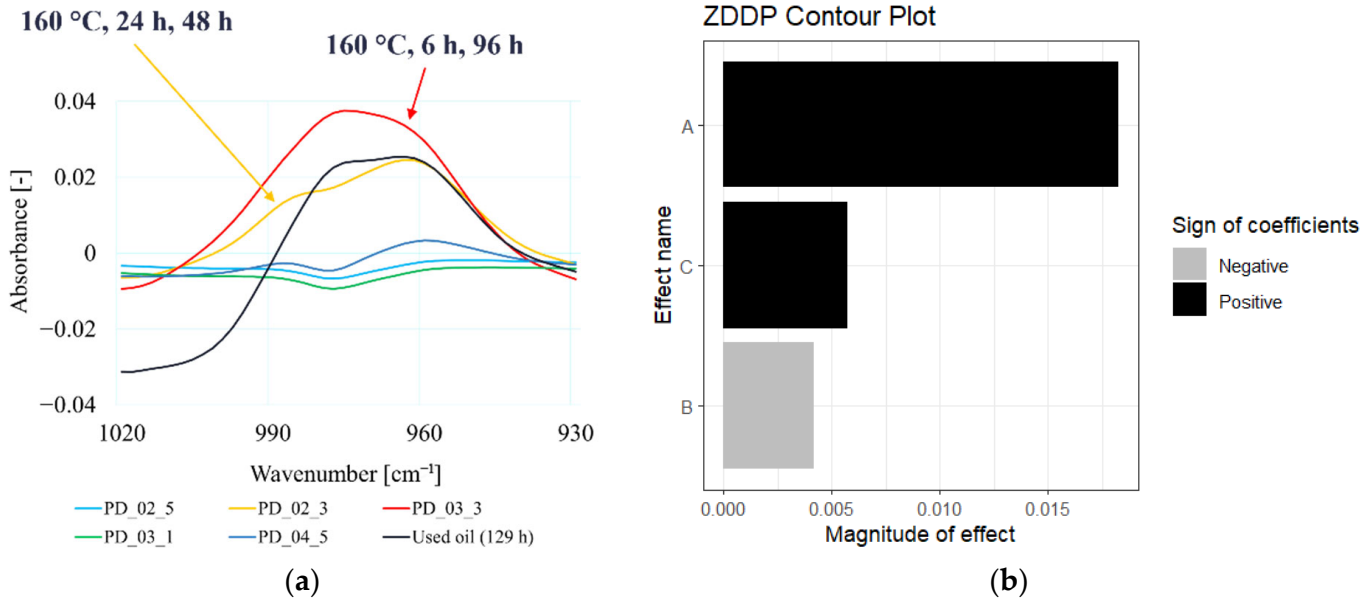


Figure 7. (**a**) Difference spectra of the investigated oils in the wavenumber range of the anti-wear additive (ZDDP); (**b**) Pareto analysis of the model constructed based on quantified changes in ZDDP content.

3.4. Gauss-Elimination Results

Analyzing the three linear models revealed that the heating period had a negligible impact on the variation in system parameters. Consequently, this factor was fixed in subsequent experiments, reducing the number of independent variables from three to two. To enhance the models, the original two-dimensional fractional factorial design was expanded by adding four axial points. These new oil samples extended the range of the investigated design space, as shown in Figure 8. However, due to the properties of the oil

used, it was not possible to identify which artificial aging setup best matched the conditions. Therefore, a new approach was taken: the linear model equations for the three response variables—(1) coefficient of friction, (2) average wear scar diameter, and (3) change in ZDDP content—were combined into a system of equations. On the left side, the model equations based on artificial aging parameters are shown, while on the right side, the values for the oil used are presented.

$$0.1342 + 0.0007(A) + 0.001(B) - 0.00365(C) = 0.127 \quad (1)$$

$$512.336 + 24.292(A) - 5.125(B) - 14.675(C) = 495.8 \quad (2)$$

$$0.0346 + 0.015(A) - 0.003458(B) + 0.003315(C) = 0.0411 \quad (3)$$

Solving this system of equations with Gauss–Jordan elimination provided an approximate artificial aging setup for the used oil, with results indicating a temperature of 132.8 °C and a total aging time of 103.1 h. However, this aging setup was not experimentally validated because the aging time was handled as a discrete variable due to equipment limitations, allowing only values divisible by 24. Despite this, applying the resulting parameters (132.8 °C, 103.1 h) in the experimental design framework enabled the identification of artificially aged oil samples that most closely resembled the used oil, as also shown in Figure 8. To verify these findings, surface analytical characterization was performed on disc specimens tested with both artificially aged oils and the used oil, as summarized in Table 3. In addition, Table 3 provides a comprehensive overview of all lubricants investigated in this study, including their properties and average wear scar diameters.

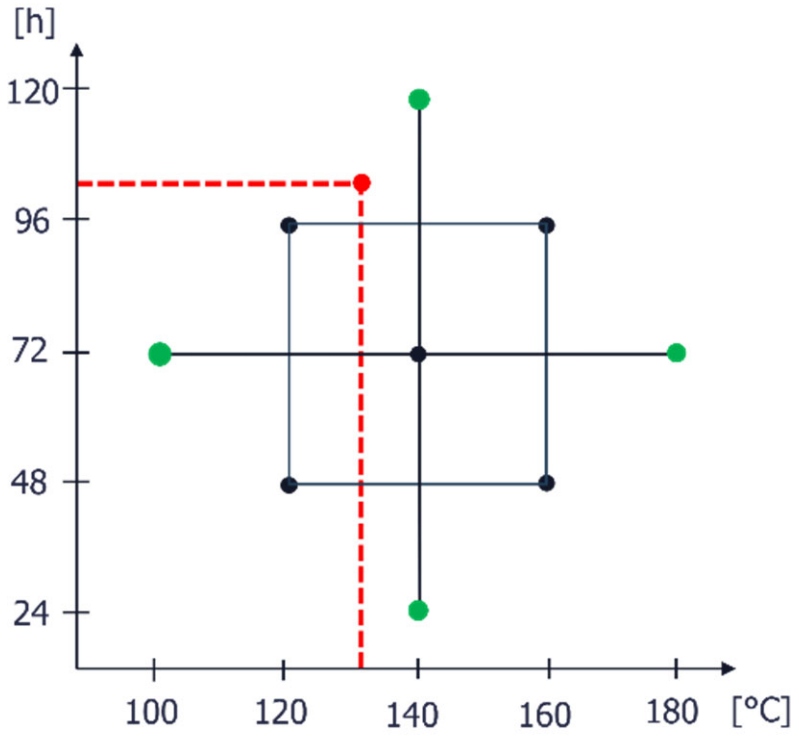


Figure 8. Two-dimensional fractional factorial design extended with the four axis points (green) and the result of the linear system of equations (red). The result of the linear system indicates the position of the used oil based on the artificial aging settings.

Table 3. Overview of all lubricant samples investigated in this study, including those selected for surface analytical evaluation.

Sample ID	Type of Oils	Oil Aging Temperature [°C]	Oil Aging Heating Period [h]	Total Oil Aging Time [h]	Average Wear Scar Diameter [µm]	Surface Analytical Evaluation
PD_02_3	Artificially aged oils	160	24	48	574.2	-
PD_02_5		120	6	48	572	-
PD_03_1		120	24	96	456.9	X
PD_03_3		160	6	96	479.6	-
PD_04_5		140	12	72	469	X
Used oil (129 h)	Used oil	~132.8 *	-	~103.1 *	495.8	X
PD_06_1	Artificially aged oils	140	12	120	495.1	X
PD_06_3		180	12	72	637.5	-
PD_06_5		140	12	24	478.3	-
PD_07_5		100	12	72	504.2	X

* Gauss-Jordan elimination results.

3.5. Surface Analysis

The aim of the surface analysis of the selected disc specimens was to examine the composition of the ZDDP-derived tribofilm formed between the contacting components. The investigation mainly focused on the two primary constituents of the ZDDP tribofilm—Zn 2p and P 2p. Figure 9 shows the variation in atomic percentage of the examined elements along the wear track of the disc specimens.

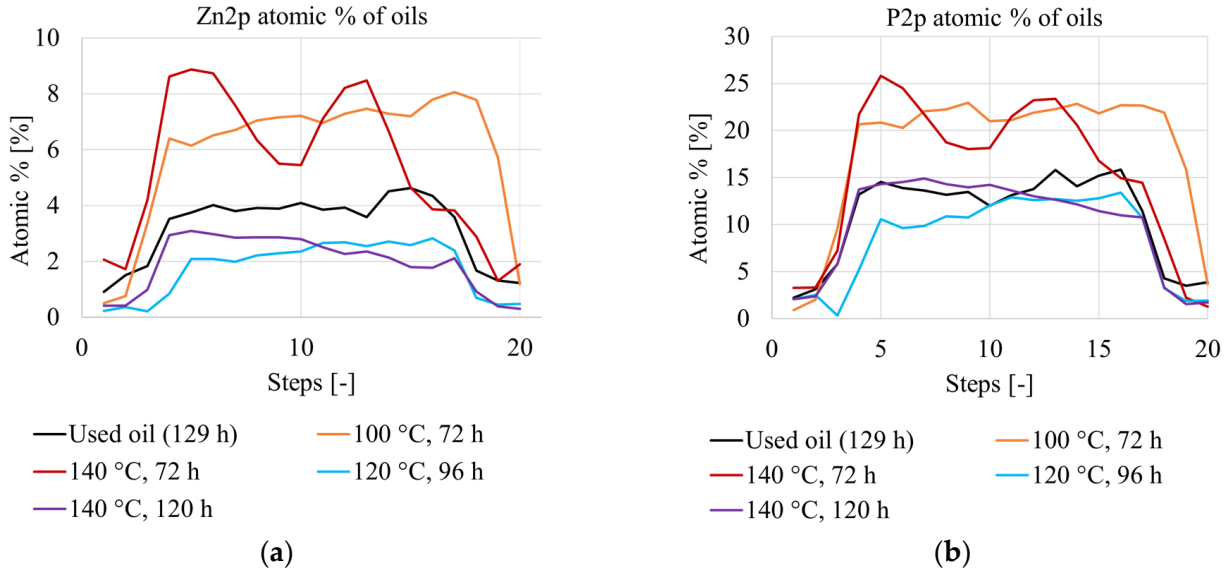


Figure 9. (**a**) XPS analysis showing the variation in atomic percentage of the Zn2p element along the wear scar of the disc specimen; (**b**) XPS analysis showing the variation in atomic percentage of the P2p element along the wear scar of the disc specimen.

Since the widths of the wear scars varied, the horizontal axis shows the steps used during line scan mode rather than the actual distance. Both Figure 9a,b illustrate that the tribofilm formed using the used oil most closely matches the composition of the artificially aged oils shown in blue (aging temperature = 120 °C, aging time = 96 h) and purple (aging temperature = 140 °C, aging time = 120 h). This aligns well with the results in Figure 8, where the used oil is also most similar to these two artificially aged oils, as determined

by the Gaussian elimination method. Although direct validation of the artificial aging process was not possible due to technological limitations, the tribofilm composition analysis effectively narrowed down the range of artificially aged oils that could be comparable to the used oil—especially when aiming to match parameters like the coefficient of friction, average wear scar diameter, and antiwear additive content.

Several studies in the literature provide useful context for interpreting the current findings. Agócs et al. reported in their field tests that, after 5000 km of operation, the phosphorus and zinc contents in the tribofilm were 8–10 atomic percent and 2–4 atomic percent, respectively. These values are similar to those measured in the used engine oil sample taken after 129 h of engine test bench operation in this study. However, with increasing mileage, these values decreased, clearly showing the gradual depletion of the ZDDP additive [41]. Dörr et al. demonstrated that artificial aging at 180 °C caused significant ZDDP degradation, with Zn and P contents in the tribofilm falling below 1 atomic percent and 2.3 atomic percent, respectively [34]. Jech et al. studied oil aging at 180 °C and found that after 8 h, the tribofilm still contained 7–8 atomic percent P and about 3 atomic percent Zn. Yet, after 50 h, the Zn level had already decreased to approximately 1 atomic percent, again indicating ZDDP depletion [33]. Thornley's studies directly compared artificially aged oils with oils obtained from field operations. The artificially aged oil produced a tribofilm about 20 nm thinner and had significantly lower elemental concentrations, with around 5% phosphorus and less than 1% zinc. In contrast, the used oil from engine operation displayed higher values, with nearly 10% phosphorus and zinc levels ranging from 3 to 4% [30]. These literature findings appear consistent with the present results, suggesting that the developed methodology may provide a suitable approach for approximating in-engine aging behavior.

4. Conclusions

In the present study, the effects of artificial oil aging parameters—namely aging temperature, aging duration, and heating cycle length—were systematically investigated using the Design of Experiments (DoE) methodology. Based on the developed linear model, the variation in heating cycle length showed a negligible impact on the results of the artificial aging process. Among the responses studied, the coefficient of friction and average wear scar diameter were most significantly influenced by aging time. At the same time, the change in antiwear additive content was primarily influenced by the aging temperature. These findings suggest that the heating cycle length can be handled as a fixed parameter in future experiments, thereby reducing the number of tests required to understand the system's behavior.

One of the objectives of this research was to determine whether it is possible to create an artificially aged lubricant with properties that closely resemble those of a used oil sample collected after 129 h of engine testing. To achieve this, the Design of Experiments (DoE) methodology was used, and the resulting linear model equations were solved using Gaussian elimination. The identified aging temperature of 132.8 °C and aging time of 103.1 h provided an approximate operational range for replicating the target oil properties. However, due to technological limitations—specifically, the artificial aging apparatus being limited to processing aging times divisible by 24—direct experimental validation of these values was not feasible. Instead, verification was performed through surface analytical examination of wear scars on disc specimens, focusing on the composition of the ZDDP-derived tribofilm formed in the contact zone. The atomic percentage distributions of Zn 2p and P 2p elements along the wear scars were analyzed for samples aged with oils exhibiting similar properties to the used oil. The results supported the hypothesis that the artificially aged oils, whose properties most closely matched those of the reference used oil, produced

comparable tribofilm characteristics. The investigated aging parameters producing the highest similarity were

- A 120 °C aging temperature and 96 h aging time;
- A 140 °C aging temperature and 120 h aging time.

Future work will focus on additional development of the aging apparatus in order to accept flexible parameters and continuous values, which would facilitate direct validation of the presented aging program. In addition, an in-depth study of the tribofilms of used and artificially aged oils by depth profiling X-ray photoelectron spectroscopy would allow the detailed comparison of the resulting boundary layers. Furthermore, the assessment of usability of the proposed aging method with various alternative fuels—e.g., butanol, methanol, ternary blends, e-fuels—is also of interest.

Author Contributions: Conceptualization, D.P. and A.L.N.; methodology, D.P. and A.L.N.; validation, D.P.; investigation, D.P.; resources, A.L.N.; writing—original draft preparation, D.P.; writing—review and editing, D.P. and A.L.N.; visualization, D.P.; supervision, A.L.N.; project administration, D.P. and A.L.N.; funding acquisition, A.L.N. All authors have read and agreed to the published version of the manuscript.

Funding: This article is published in the framework of the project "Production and Validation of Synthetic Fuels in Industry-University Collaboration", project number "ÉZFF/956/2022-ITM_SZERZ". This study was partially supported by the EKÖP-24-3-I-SZE-76 UNIVERSITY RESEARCH FELLOWSHIP PROGRAM of the Ministry for Culture and Innovation from the source of the National Research, Development and Innovation Fund.

Institutional Review Board Statement: This study does not concern ethical questions related to experimentation on humans and animals.

Informed Consent Statement: No personal data was collected during the experiments.

Data Availability Statement: Data for the study are available upon request from the corresponding author.

Acknowledgments: The authors would like to express their gratitude to Márkó Kovács for his support.

Conflicts of Interest: The authors declare no conflicts of interest. The funders had no role in the design of the study, in the collection, analysis, or interpretation of data, in the writing of the manuscript, or in the decision to publish the results.

Abbreviations

The following abbreviations are used in this manuscript:

AWSD	Average wear scar diameter
CoF	Coefficient of friction
DoE	Design of experiment
E20	20% ethanol and 80% gasoline (petrol)
FT-IR	Fourier-transform infrared spectrometer
XPS	X-ray photoelectron spectrometer
ZDDP	Zinc dialkyldithiophosphate antiwear additive

References

1. Macharia, V.M.; Garg, V.K.; Kumar, D. A review of electric vehicle technology: Architectures, battery technology and its management system, relevant standards, application of artificial intelligence, cyber security, and interoperability challenges. *IET Electr. Syst. Transp.* **2023**, *13*, e12083. [CrossRef]
2. Öörni, R. Barriers to Adoption of a Fully Electric Vehicle—A Study of Car Users in the Helsinki Region. In *Transport Research Arena Conference*; Springer Nature: Cham, Switzerland, 2024; pp. 633–639. [CrossRef]

3. Shamsuddoha, M.; Nasir, T. The Road Ahead for Hybrid or Electric Vehicles in Developing Countries: Market Growth, Infrastructure, and Policy Needs. *World Electr. Veh. J.* **2025**, *16*, 180. [CrossRef]
4. European Comission: Emissions in the Automotive Sector. Available online: https://single-market-economy.ec.europa.eu/sectors/automotive-industry/environmental-protection/emissions-automotive-sector_en (accessed on 20 July 2025).
5. Namar, M.M.; Jahanian, O.; Shafaghat, R.; Nikzadfar, K. Engine Downsizing; Global Approach to Reduce Emissions: A World-Wide Review. *HighTech Innov. J.* **2021**, *2*, 384–399. [CrossRef]
6. International Council on Clean Transportation (ICCT). European Vehicle Market Statistics: Pocketbook 2019/20. Available online: https://theicct.org/sites/default/files/publications/European_vehicle_market_statistics_20192020_20191216.pdf (accessed on 20 July 2025).
7. Kumar, S.; Goga, G. Emission characteristics & performance analysis of a diesel engine fuelled with various alternative fuels—A review. *Mat. Today Proc.* **2023**, *in press*. [CrossRef]
8. Awogbemi, O.; Kallon, D.V.V.; Onuh, E.I.; Aigbodion, V.S. An Overview of the Classification, Production and Utilization of Biofuels for Internal Combustion Engine Applications. *Energies* **2021**, *14*, 5687. [CrossRef]
9. Chybowski, L.; Wójcik, W.; Szczepanek, M. Evaluation of Rheological and Lubrication Properties of Selected Alcohol Fuels. *Energies* **2025**, *18*, 1038. [CrossRef]
10. Aguilar-Rosas, O.A.; Farfan-Cabrera, L.I.; Erdemir, A.; Cao-Romero-Gallegos, J.A. Electrified four-ball testing–A potential alternative for assessing lubricants (E-fluids) for electric vehicles. *Wear* **2023**, *522*, 204676. [CrossRef]
11. Xu, Y.; Zheng, Q.; Geng, J.; Dong, Y.; Tian, M.; Yao, L.; Dearn, K.D. Synergistic effects of electroless piston ring coatings and nano-additives in oil on the friction and wear of a piston ring/cylinder liner pair. *Wear* **2019**, *422*, 201–211. [CrossRef]
12. Paulovics, L.; Kuti, R.; Rohde-Brandenburger, J.; Tóth-Nagy, C. Development of comparative investigation method for timing chain wear analysis using oscillating tribometer. *Acta Tech. Jaurinensis* **2021**, *14*, 406–423. [CrossRef]
13. Dörr, N.; Agocs, A.; Besser, C.; Ristic, A.; Frauscher, M. Engine Oils in the Field: A Comprehensive Chemical Assessment of Engine Oil Degradation in a Passenger Car. *Trib. Lett.* **2019**, *67*, 68. [CrossRef]
14. Agocs, A.; Nagy, A.L.; Tabakov, Z.; Perger, J.; Rohde-Brandenburger, J.; Schandl, M.; Besser, C.; Dörr, N. Comprehensive assessment of oil degradation patterns in petrol and diesel engines observed in a field test with passenger cars–Conventional oil analysis and fuel dilution. *Tribol. Int.* **2021**, *161*, 107079. [CrossRef]
15. *CEC L-48-A00*; Oxidation Stability of Lubricating Oils Used in Automotive Transmissions by Artificial Ageing. Co-Ordinating European Council for the Development of Performance Tests for Fuels. Lubricants and other Fluids: Brussels, Belgium, 2014.
16. *ASTM D 6186*; Standard Test Method for Oxidation Induction Time of Lubricating Oils by Pressure Differential Scanning Calorimetry (PDSC). ASTM International: West Conshohocken, PA, USA, 2013.
17. *ASTM D 943*; Standard Test Method for Oxidation Characteristics of Inhibited Mineral Oils. ASTM International: West Conshohocken, PA, USA, 2017.
18. *ASTM D 2272*; Standard Test Method for Oxidation Stability of Steam Turbine Oils by Rotating Pressure Vessel. ASTM International: West Conshohocken, PA, USA, 2014.
19. Nagy, A.L.; Rohde-Brandenburger, J.; Zsoldos, I. Artificial Aging Experiments of Neat and Contaminated Engine Oil Samples. *Lubricants* **2021**, *9*, 63. [CrossRef]
20. Steinschütz, K.; Geringer, B.; Jech, M.; Urbanek, M.; Wopelka, T.; Besser, C. *Impact of Oil Aging on Wear of Piston Ring and Cylinder Liner System 2010-32-0124*; SAE Technical Paper: Warrendale, PA, USA, 2010. [CrossRef]
21. Motamen Salehi, F.; Morina, A.; Neville, A. The effect of soot and diesel contamination on wear and friction of engine oil pump. *Tribol. Int.* **2017**, *115*, 285–296. [CrossRef]
22. Besser, C.; Agocs, A.; Ristic, A.; Frauscher, M. Implementation of Nitration Processes in Artificial Ageing for Closer-to-Reality Simulation of Engine Oil Degradation. *Lubricants* **2022**, *10*, 298. [CrossRef]
23. Fuller, M.L.S.; Kasrai, M.; Bancroft, G.M.; Fyfe, K.; Tan, K.H. Solution decomposition of zinc dialkyl dithiophosphate and its effect on antiwear and thermal film formation studied by X-ray absorption spectroscopy. *Tribol. Int.* **1998**, *31*, 627–644. [CrossRef]
24. Uy, D.; Simko, S.J.; Carter, R.O., III; Jensen, R.K.; Gangopadhyay, A.K. Characterization of anti-wear films formed from fresh and aged engine oils. *Wear* **2007**, *263*, 1165–1174. [CrossRef]
25. Cen, H.; Morina, A.; Neville, A. Effect of lubricant ageing on lubricants' physical and chemical properties and tribological performance; Part I: Effect of lubricant chemistry. *Ind. Lubr. Tribol.* **2018**, *70*, 385–392. [CrossRef]
26. Besser, C.; Agocs, A.; Ronai, B.; Ristic, A.; Repka, M.; Jankes, E.; McAleese, C.; Dörr, N. Generation of engine oils with defined degree of degradation by means of a large scale artificial alteration method. *Tribol. Int.* **2019**, *132*, 39–49. [CrossRef]
27. Spikes, H. Mechanisms of ZDDP—An update. *Tribol. Lett.* **2025**, *73*, 38. [CrossRef]
28. Ueda, M.; Kadiric, A.; Spikes, H. On the crystallinity and durability of ZDDP tribofilm. *Tribol. Lett.* **2019**, *67*, 123. [CrossRef]
29. Hsu, C.J.; Barrirero, J.; Merz, R.; Stratmann, A.; Aboulfadl, H.; Jacobs, G.; Gachot, C. Revealing the interface nature of ZDDP tribofilm by X-ray photoelectron spectroscopy and atom probe tomography. *Ind. Lubr. Tribol.* **2020**, *72*, 923–930. [CrossRef]

30. Thornley, A. The Interactions of Surface-Active Engine Oil Additives in Low Viscosity Engine Oils and Their Effect on Tribological Performance. Doctoral Thesis, University of Leeds, Leeds, UK, 2023.
31. Thersleff, T.; Jenei, I.Z.; Budnyk, S.; Dorr, N.; Slabon, A. Soot nanoparticles generated from tribofilm decomposition under real engine conditions for identifying lubricant hazards. *ACS Appl. Nano Mater.* **2020**, *4*, 220–228. [CrossRef]
32. Agocs, A.; Frauscher, M.; Ristic, A.; Dörr, N. Impact of soot on internal combustion engine lubrication—Oil condition monitoring, tribological properties, and surface chemistry. *Lubricants* **2024**, *12*, 401. [CrossRef]
33. Jech, M.; Hofer, A.; Tomastik, C.; Wopelka, T.; Gachot, C. Influence of artificially altered engine oil on tribofilm formation and wear behaviour of grey cast cylinder liners. *Lubricants* **2023**, *11*, 476. [CrossRef]
34. Dörr, N.; Brenner, J.; Ristić, A.; Ronai, B.; Besser, C.; Pejaković, V.; Frauscher, M. Correlation between engine oil degradation, tribochemistry, and tribological behavior with focus on ZDDP deterioration. *Tribol. Lett.* **2019**, *67*, 62. [CrossRef]
35. Dudás, A.; Laki, G.; Nagy, A.L.; Zsoldos, I.; Hanula, B.; Bartel, D. Wear behaviour of ceramic particle reinforced atmospheric plasma spray coatings on the cylinder running surface of internal combustion engines. *Wear* **2022**, *502*, 204373. [CrossRef]
36. Nagy, A.L. Development of an artificial aging process for automotive lubricants. In Proceedings of the Spring Wind, Debrecen, Hungary, 3–5 May 2019; pp. 771–775.
37. *ISO 19291:2016(E)*; Lubricants—Determination of Tribological Quantities for Oils and Greases—Tribological Test in the Translator Oscillation Apparatus. International Organization for Standardization: Geneva, Switzerland, 2016.
38. Hamrock, B.J.; Dowson, D. Isothermal Elastohydrodynamic Lubrication of Point Contacts, Part III—Fully Flooded Results. *J. Lubr. Technol.* **1977**, *99*, 264–276. [CrossRef]
39. *ASTM D7042-21*; Standard Test Method for Dynamic Viscosity and Density of Liquids by Stabinger Viscometer (and the Calculation of Kinematic Viscosity). ASTM International: West Conshohocken, PA, USA, 2021.
40. *ASTM E2412-10(2018)*; Standard Practice for Condition Monitoring of In-Service Lubricants by Trend Analysis Using Fourier Transform Infrared (FT-IR) Spectrometry. ASTM International: West Conshohocken, PA, USA, 2018.
41. Agocs, A.; Besser, C.; Brenner, J.; Budnyk, S.; Frauscher, M.; Dörr, N. Engine oils in the field: A comprehensive tribological assessment of engine oil degradation in a passenger car. *Tribol. Lett.* **2022**, *70*, 28. [CrossRef]

Disclaimer/Publisher's Note: The statements, opinions and data contained in all publications are solely those of the individual author(s) and contributor(s) and not of MDPI and/or the editor(s). MDPI and/or the editor(s) disclaim responsibility for any injury to people or property resulting from any ideas, methods, instructions or products referred to in the content.